OBJECT CORRELATION AND MANEUVER DETECTION USING OPTIMAL CONTROL PERFORMANCE METRICS

Marcus Holzinger
Graduate Research Assistant, Aerospace Engineering Sciences
University of Colorado at Boulder
Daniel Scheeres
Professor, Seebass Chair, Aerospace Engineering Sciences
University of Colorado at Boulder

Abstract

Object correlation and maneuver detection are persistent problems in space surveillance and space object catalog maintenance. This paper demonstrates the utility of using quadratic trajectory control cost, an analog to the trajectory L_2-norm in control, as a distance metric with which to both correlate object tracks and detect maneuvers using Uncorrelated Tracks (UCTs), real-time sensor measurement residuals, and prior state uncertainty. State and measurement uncertainty are incorporated into the computation, and distributions of optimal control usage are computed. Both UCT correlation as well as maneuver detection are demonstrated in several scenarios Potential avenues for future research and contributions are summarized.

1 INTRODUCTION

The problem of properly correlating on-orbit object observations and detecting object maneuvers is a challenging and persistent endeavor. There are currently at least 19,000 trackable on-orbit objects, 1,300 of which are active [1], and these numbers are expected to grow significantly due to increasing tracking capabilities and new launches [2]. Predicting conjunction events is a difficult task [3], however recent events highlight the mutual interest that national and private operators share for accurate object correlation and maneuver detection capability [4].

Object track correlation in space operations is distinct from real-time track correlation, as in Resident Space Object (RSO) track correlation there are large gaps in observations (hours to weeks), with each observation track being relatively dense in terms of measurements. This is contrasted with multi-target, multi-sensor tracking and target association commonly encountered in real-time applications [5], where measurements are made much faster than the system dynamics change.

The problem of correlating Uncorrelated Tracks (UCTs) over large time periods is particularly difficult when objects maneuver during gaps in observations. Even relatively small stationkeeping maneuvers at Geostationary Earth Orbit (GEO) can result in position discrepancies of many kilometers after an observation gap of several days. UCT correlation is further confounded by state estimate uncertainties. Because both the initial and final UCTs are best estimates and possess associated uncertainty distributions, the question of correlation becomes inherently difficult to answer in operational settings, particularly in regions of space that have particularly dense spacecraft populations.

Given a propagated best estimate and associated distribution, correlating UCTs essentially asks whether a newly observed object (with an associated distribution) can possibly be a previously observed object, and if not, what the 'distance' discrepancy is. There are many distance- or pseudo-distance metrics that may be used to measure the distance between two state distributions. These include the Mahalonobis (M)-Distance, the Kullback-Leibler (KL)-Distance [6], the Bhattacharyya (B)-Distance [7], and the Maximum a Posteriori (MaP)-Distance (also known as Baysean) . All of these measures quantify a distance- or pseudo-distance

metric in the presence of uncertainty, and are typically applied to the state difference between a predicted object state and the best estimate of the newly observed object state.

Problematically, it remains that none of the M-, KL-, B-, or MaP-distance metrics, when applied to state distributions, directly quantifies the level of propulsive effort required to effect the state change given a gap in observation. This difference is critical as very small fuel expenditures at specific points in an orbit can produce outsized state discrepancies. Further, as on-board fuel remains a scarce commodity for operational spacecraft, satellite operators are likely to execute optimal or near-optimal maneuvers.

This paper applies a previously developed approach [8] to compute control distance metric distributions, analogous to ΔV distributions, for both UCT correlation as well as maneuver detection. In particular, several example scenarios are generated to emphasize the applicability of the approach to Space Situational Awareness (SSA).

Organization of the paper is as follows: the approaches for both object correlation and maneuver detection are summarized from previous work and their applicability is discussed. Several scenarios are motivated based on GEO object cross-tagging and maneuver detection applications. The described methodology is then applied to the scenarios, illustrating how control distance metrics may be used to correlate objects and detect maneuvers, as well as potentially characterize objects. Finally conclusions and future work are discussed.

2 THEORY

The background theory for both control-effort based object correlation and maneuver detection is largely developed in [8]. The authors suggest a thorough reading of [8] for the interested reader. The results for object correlation and maneuver detection are summarized individually in the following subsections. While the focus of this effort is on orbit dynamics, generality is maintained in the derivations making the approach valid for systems with dynamics $\dot{\mathbf{x}} = \mathbf{f}(\mathbf{x}, \mathbf{u}, t)$ with $\mathbf{x} \in \mathbb{R}^n$, $\mathbf{u} \in \mathbb{R}^m$, and $t \in [t_0, t_f]$, $t_0 < t_f$.

2.1 Control Effort as a Metric

As mentioned in the introduction, satellite operators are loathe to expend unnecessary quantities of fuel to effect maneuvers. Both the UCT correlation and maneuver detection approaches are posed in terms of optimal control problems, so it is sensible to determine an appropriate performance function P. The function chosen is

$$P = \frac{1}{2}\int_{t_0}^{t_f} \mathcal{L}_u(\mathbf{x}(\tau), \mathbf{u}(\tau), \tau) d\tau = \frac{1}{2}\int_{t_0}^{t_f} \mathbf{u}(\tau)^T \mathbf{u}(\tau) d\tau \tag{1}$$

Subject to dynamics $\dot{\mathbf{x}} = \mathbf{f}(\mathbf{x}, \mathbf{u}, t)$ with $\mathbf{x} \in \mathbb{R}^n$, $\mathbf{u} \in \mathbb{R}^m$, and $t \in [t_0, t_f]$. This performance function is similar to an energy measure and is analogous to the L_2 control distance norm

$$P_{L_2} = \sqrt{2P} = \|\mathbf{u}(t)\|_{L_2} = \left(\int_{t_0}^{t_f} \mathbf{u}(\tau)^T \mathbf{u}(\tau) d\tau\right)^{\frac{1}{2}}$$

which is a classic example of an L_2 norm [9]. By inspection it is clear that any optimal trajectory $(\mathbf{x}^*, \mathbf{u}^*)$ that minimizes P also minimizes the L_2-norm $P_{L_2} = \sqrt{2P}$. Minimum $P_{\Delta V}$ (fuel) problems are much more involved to solve than minimum energy analogs such as P as they necessarily involve periods of maximum thrust and drifting. This introduces significant complication when the boundary conditions of the problem are considered random variables, so for this present work the L_2-analog performance function P is used. It can be shown using the Cauchy-Schwartz inequality [10] that the performance functions P and P_{L_2} bound ΔV_{LQ} from above:

$$\Delta V_{LQ} \leq \sqrt{t_f - t_0} P_{L_2} = \sqrt{t_f - t_0}\sqrt{2P} \tag{2}$$

Thus, the performance function P, an energy cost analog, can produce an upper conservative bound on the possible fuel cost distribution. Using P defined in (1) as the performance function metric has the additional benefit that the control authority u_m of the object in question need not be known.

2.2 Object Correlation Using Minimum Control Effort Distributions

The problem under consideration is illustrated in Fig. 1. An initial object track consisting of a sequence of observations ultimately produces a state estimate $\mathbf{x}_0$ and an associated estimate covariance $\mathbf{P}_0$ (corresponding to some arbitrary time t_0). We define this track UCT_0 as the triplet $(t_0, \mathbf{x}_0, \mathbf{P}_0)$. At some later time t_f, a new object track is initiated based on new observations. After all of the new observations are collected an estimate of the state and covariance from when the new track was first started (at time t_f) can be generated, creating the new UCT_f triplet $(t_f, \mathbf{x}_f, \mathbf{P}_f)$. Estimation theory typically used in to generate UCTs can be found in Tapley [11].

Supposing now that multiple initial and final UCTs exist, we are faced with the problem of determining which UCTs should be associated (or 'paired') with one another. One way to do this is do compute a measure of how 'expensive' a maneuver between UCTs would be. A logical assumption would be that UCTs with the smallest required connecting control effort should be paired to one another, as on-orbit fuel is such a scarce commodity. This concept is very similar to comparing differences in propagated homogeneous states $\mathbf{x}_{f,p}$ to new UCT states $\mathbf{x}_f$, as if $\mathbf{x}_{f,p} \approx \mathbf{x}_f$, the minimum optimal control is necessarily $\mathbf{u}^*(t) \approx \mathbf{0}$. Because the approach essentially solves the Two-Point Boundary Value Problem (TPBVP) with uncertain boundary conditions, it is also called the Uncertain Two-Point Boundary Value Problem (UTPBVP).

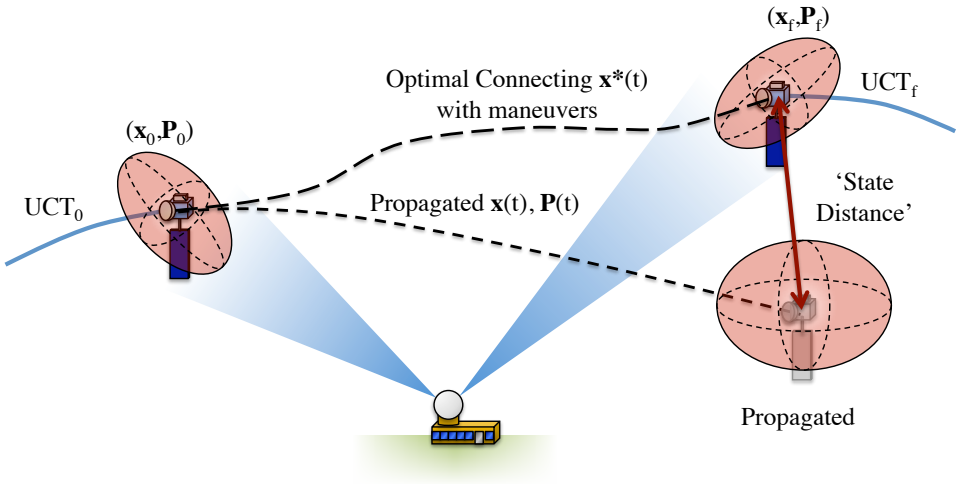

Figure 1: Problem Illustration

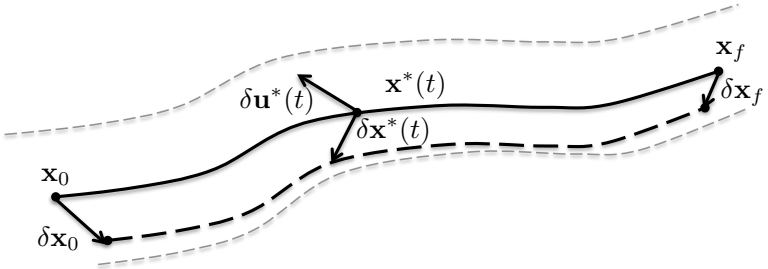

Figure 2: Trajectory variations in the UTPBVP

After an optimal connecting trajectory $(\mathbf{x}^*, \mathbf{u}^*)$ is found, the surrounding region is linearized and variations of the boundary condition are considered, as shown in Fig. 2. The boundary conditions are then

treated as random variables where $\delta\mathbf{Z}^T = \left[\delta\mathbf{X}_0^T \;\; \delta\mathbf{X}_f^T\right] \in \mathbb{R}^{2n}$,

$$\mathbb{E}\left[\delta\mathbf{Z}\right] = \mathbf{0} \tag{3}$$

$$\mathbb{E}\left[\delta\mathbf{Z}\delta\mathbf{Z}^T\right] = \mathbf{P}_z = \begin{bmatrix} \mathbf{P}_0 & \mathbf{0} \\ \mathbf{0} & \mathbf{P}_f \end{bmatrix} \tag{4}$$

With Gaussian boundary condition distributions the distribution of the performance metric P may be written as

$$P = P_n + \omega(t_f, t_0)^T\delta\mathbf{Z} + \delta\mathbf{Z}^T\mathbf{\Omega}(t_f, t_0)\delta\mathbf{Z} \tag{5}$$

The parameter $P_n > 0 \in \mathbb{R}$ is the nominal value of the performance function in the absence of uncertainty and $\omega(t_f, t_0) \in \mathbb{R}^{2n}$ and $\mathbf{\Omega}(t_f, t_0) \in \mathbb{R}^{2n\times 2n}$ are linear and quadratic terms with respect to $\delta\mathbf{Z}$ that capture the optimal control policy and linearized dynamics about the nominal connecting trajectory $(\mathbf{x}^*(t), \mathbf{u}^*(t))$. With (5) it is clear that if there is no uncertainty in the system, $P \to P_n$ is deterministic. Conversely, if $P_n = 0$, then P will always have some positive control distance distribution comensurate to the level of uncertainty in the boundary conditions. In other words, even for nominal homogeneous connecting trajectories, the boundary condition uncertainty means the probability of the actual connecting trajectory being exactly homogeneous is precisely zero.

2.3 Maneuver Detection Using Minimum Control Effort Distributions

Fig. 3 describes elements composing the Measurement Residual Boundary Value Problem (MRBVP) approach. At time t_0 the previous observation ends and an observation gap begins. The nominal state $\mathbf{x}_0 = \mathbf{x}(t_0)$ and uncertainty $\mathbf{P}_0 = \mathbf{P}(t_0)$ is propagated over the interval $t \in [t_0, t_f]$ to time t_f, generating the homogeneous state $\mathbf{x}_h$ and uncertainty $\mathbf{P}_h$. The expected measurement is computed using the sensor measurement model to be $\mathbf{y} = \mathbf{h}(\mathbf{x}_h)$. The sensor measurement $\mathbf{y}_m$ is taken, and the measurement residual is defined as $\delta\mathbf{y} = \mathbf{y}_m - \mathbf{y} = \mathbf{y}_m - \mathbf{h}(\mathbf{x}_h)$. The space surrounding the nominal connecting trajectory $\mathbf{x}_h(t)$ is linearized, and the measurement residual is decomposed into three constituent residuals due to 1) state uncertainty in $\delta\mathbf{x}_h$, 2) sensor uncertainty η_m, and 3) state deviations due to active control $\delta\mathbf{x}_{u,f}$. The linearization is written as

$$\mathbf{y}_m \approx \mathbf{y} + \delta\mathbf{y} = \mathbf{h}(\mathbf{x}_h) + \frac{\partial\mathbf{h}}{\partial\mathbf{x}_h}\delta\mathbf{x}_h + \frac{\partial\mathbf{h}}{\partial\mathbf{x}_h}\delta\mathbf{x}_{u,f} + \eta_m$$

For homogeneous trajectories about the trajectory linearization without process noise the final state deviation $\delta\mathbf{x}_h$ may be written in terms of the initial state deviation as $\delta\mathbf{x}_h = \mathbf{\Phi}_{xx}(t_f, t_0)\delta\mathbf{x}_0$. Defining $\mathbf{H} = \partial\mathbf{h}/\partial\mathbf{x}_h$ and observing that $\mathbf{y} = \mathbf{h}(\mathbf{x}_h)$, the residual is defined in the local linearization about $\mathbf{x}_h$ as

$$\delta\mathbf{y} = \mathbf{H}\mathbf{\Phi}_{xx}(t_f, t_0)\delta\mathbf{x}_0 + \mathbf{H}\delta\mathbf{x}_{u,f} + \eta_m \tag{6}$$

Note that in traditional applications without a state deviation due to control ($\delta\mathbf{x}_{u,f} = \mathbf{0}$), the expected variance of the measurement residual is

$$\begin{aligned} \mathrm{Var}[\delta\mathbf{y}_h] = \mathbf{P}_{y,h} &= \mathbb{E}\left[\delta\mathbf{y}_h\delta\mathbf{y}_h^T - \mathbb{E}\left[\delta\mathbf{y}_h\right]\mathbb{E}\left[\delta\mathbf{y}_h\right]^T\right] \\ &= \mathbb{E}\left[\mathbf{H}\mathbf{\Phi}_{xx}(t_f, t_0)\delta\mathbf{x}_0\delta\mathbf{x}_0^T\mathbf{\Phi}_{xx}(t_f, t_0)^T\mathbf{H}^T + \mathbf{H}\mathbf{\Phi}_{xx}(t_f, t_0)\delta\mathbf{x}_0\eta_m^T + \eta_m\eta_m^T\right] \\ &= \mathbf{H}\mathbf{\Phi}_{xx}(t_f, t_0)\mathbf{P}_0\mathbf{\Phi}_{xx}(t_f, t_0)^T\mathbf{H}^T + \mathbf{R} \end{aligned}$$

where $\mathbb{E}\left[\delta\mathbf{x}_0\delta\mathbf{x}_0^T\right] = \mathbf{P}_0$ and $\mathbb{E}\left[\eta_m\eta_m^T\right] = \mathbf{R}$. $\mathbf{P}_{y,h}$ is the Kalman filter pre-update measurement residual covariance, and is often used in conjunction with the Mahalanobis distance to determine whether a new measurement is statistically probable given the filters measurement and dynamic models.

In the case of optical measurements (azimuth β and elevation γ), Fig. 3 can be viewed in the measurement space as shown in Fig. 4

In this formulation the performance metric distribution under optimal control is

$$P = \delta\mathbf{y}^T\mathbf{G}_{yy}\delta\mathbf{y} + \delta\mathbf{y}^T\mathbf{G}_{yw}\delta\mathbf{W} + \delta\mathbf{W}^T\mathbf{G}_{ww}\delta\mathbf{W} \tag{7}$$

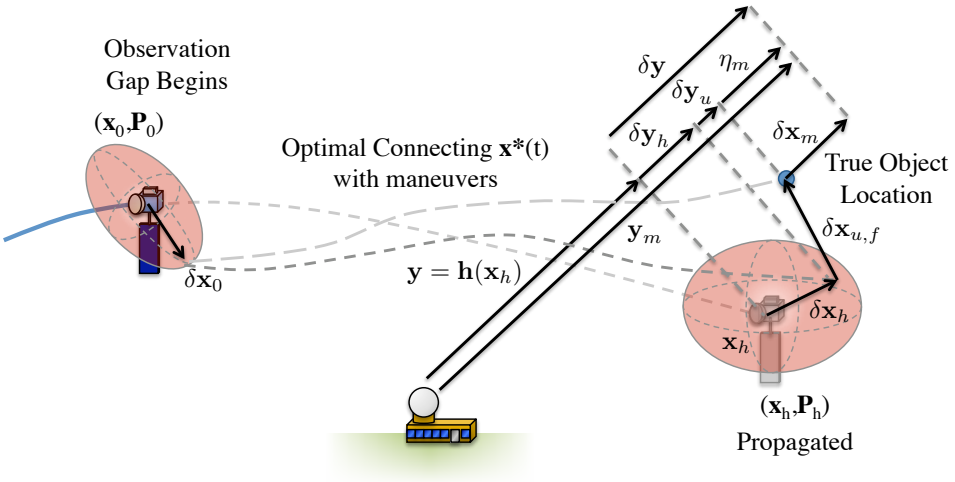

Figure 3: Problem Definition and Measurement Model

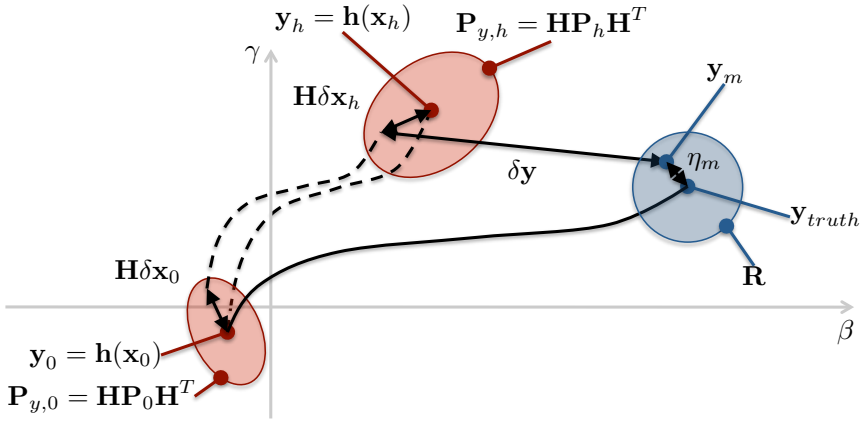

Figure 4: MRBVP Illistration for an optical sensor using azimuth (β) and elevation (γ).

where $\delta\mathbf{y} = \mathbf{y}_m - \mathbf{h}(\mathbf{x}_h)$ is the measurement residual (consistent with standard nonlinear batch and EKF definitions), $\delta\mathbf{W}^T = \left[\delta\mathbf{X}_0^T \ \eta_m^T\right]$ captures the inital state and measurement uncertainty, and $\mathbf{G}_{yy}$, $\mathbf{G}_{yw}$, and $\mathbf{G}_{ww}$ are linear and quadratic coupling terms. In a manner similar to the UTPBVP performance metric distribution (5), the MRBVP control metric distribution (7) contains both deterministic elements ($\delta\mathbf{y}$) and random variables ($\delta\mathbf{W}$). As $\delta\mathbf{y} \to \mathbf{0}$, the observation occurs exactly where it is expected, however (7) captures the effective additional control effort necessitated by the initial state and measurement uncertainty ($\delta\mathbf{W}$). Similarly, if $\delta\mathbf{W} \to \mathbf{0}$, the system becomes completely deterministic and is purely a function of the measurement residual.

2.4 UTPBVP and MRBVP Utility

Both the UTPBVP approach to object correlation and MRBVP approach to maneuver detection are fundamentally derived using optimal control to minimize the control distance metric P shown in (1). Further, due to the calculus of variations approach, boundary condition uncertainty is directly accounted for. Despite the similarities in their derivations, the utility of either approach is very different.

For the purposes of object correlation, the UTPBVP approach in §2.2 allows operators to select sets

of inital and final UCTs and compute corresponding connecting trajectory control distance distributins. Once these are computed, the operator may make decisions concerning which candidate UCT pairing is most likely. Further, because the distributions have a basis in rigorous optimal control theory and the performance function serves as an upper bound on ΔV expenditures, realistic distributions of ΔV usage may be inferred.

The utility of the MRBVP problem is somewhat different. Instead of being used to correlate objects, the MRBVP approach in §2.3 may be used after an observation gap to immediately determine the distribution of possible optimal maneuvers occurring during the observation gap. This computation also benefits from having a rigorous optimal control-based derivation and control distance metric bounding, allowing the resulting conservative distribution of ΔV usage to supply object characterization data. It should also be further stressed that this algorithm is used with the first new measurement after an observation gap, providing maneuver characterization immediately upon track acquisition.

The utility of the approaches is now demonstrated in the following Scenario section.

3 SCENARIOS

3.1 Scenario 1: Geostationary Cluster Cross-Tagging

This example is inspired by Intelsat constellation TLE cross-tagging [14]. The scenario involves a two-spacecraft cluster in GEO in which the first spacecraft executes a small maneuver ($\text{UCT}_{0,1}$ executes a 5 m/s impulsive maneuver in the inertial z direction). It is assumed that each spacecraft has been tracked long enough before the maneuver so that they have nominal pre-maneuver ephemeris estimates. Because changes in observation angles may not be significant during or immediately after an orbit maintenance maneuver at GEO, this scenario assumes that the maneuver occurs late in the observation period. New observations are made starting the next available observation period, approximately 14 hours later and continue over the next several days. Collected observations are used to generate post-maneuver UCTs for both spacecraft. After both the initial and final UCTs are formed the objective is then to compute the control distance distributions for each individual association as well as the combined control distance distributions for mutually exclusive cases.

Table 1 shows the initial orbit elements, Table 2 shows the uncertainties for each UCT, and Table 3 describes the mutually exclusive association combinations to be examined. Note that the velocity uncertainties in all of the UCTs are nearly the same size as the magnitude of the maneuver. The nominal adjoints $\mathbf{p}_n(t)$ were found using a shooting-based Newton-method descent and the control distance distributions were computed using Pearson's Approximation. Fig. 5 depicts the optimal connecting trajectories between each combination of initial and final UCTs. Fig. 6(a) shows the associated control distance metric distribution for each combination and Fig. 6(b) shows the combined control metric distributions for each mutually exclusive case.

Table 1: Initial orbit elements for both satellites for Example 1

$\mathbf{oe}$	$\mathbf{oe}_{0,1}$	$\mathbf{oe}_{0,2}$
a (km)	42,086	42,086
e ()	0.0005	0.0005
i (deg)	0.05	0.05
Ω (deg)	0	0
ω (deg)	0	0
f (deg)	0	-0.05

Examining Fig. 6(a) it is clear that connecting either $\text{UCT}_{0,1}$ or $\text{UCT}_{0,2}$ to $\text{UCT}_{f,1}$ (the final state following the 5 m/s ΔV inclination maneuver) pushes the control distance distributions right by approximately 5 m/s, as well as further diffuses the distribution. This is as expected as $\text{UCT}_{f,1}$ possesses larger uncertainties in both position and velocity. There is no large difference due to changes in the along-track direction when

Table 2: Geostationary cluster Initial and final UCT Uncertainties for Example 1

ECI Std. Dev.	$\text{UCT}_{0,1}$	$\text{UCT}_{0,2}$	$\text{UCT}_{f,1}$	$\text{UCT}_{f,2}$
σ_x (m)	100	100	100	100
σ_y (m)	100	100	150	100
σ_z (m)	100	100	150	100
$\sigma_{\dot{x}}$ (m/s)	1.0	1.0	2.0	1.0
$\sigma_{\dot{y}}$ (m/s)	2.0	2.0	2.5	2.0
$\sigma_{\dot{z}}$ (m/s)	2.0	2.0	2.5	2.0

Table 3: Object association case descriptions for Example 1

Case	**Associations**
1	$\text{UCT}_{0,1} \rightarrow \text{UCT}_{f,1}$ $\text{UCT}_{0,2} \rightarrow \text{UCT}_{f,2}$
2	$\text{UCT}_{0,1} \rightarrow \text{UCT}_{f,2}$ $\text{UCT}_{0,2} \rightarrow \text{UCT}_{f,1}$

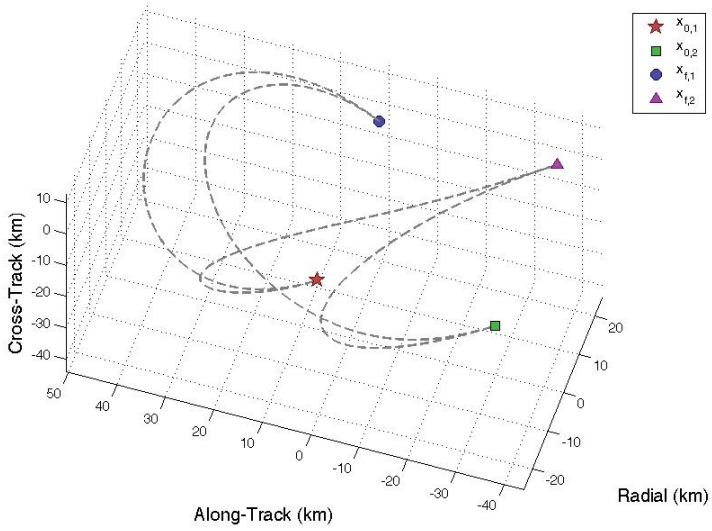

Figure 5: Candidate optimal connecting trajectories in a rotating Hill frame (circular reference orbit, $a =$ 42,086 km, $i = 0$ deg)

compared to the rather large inclination maneuver. However, the control distance metric differential due to the combined along-track maneuver is large enough for Fig. 6(b) to exhibit a lower cost for Case 1 (as found by applying Stochastic Dominance [13]), which we know to be the truth. Examining the CDF shown in Fig. 6(b) also indications that mean ΔV distance is slightly less than 14 m/s. While at first this seems large with respect to the known size of the impulse (5 m/s), it is important to realize that the mean control metric distance of 14 m/s is for all possible combinations of boundary conditions, each of which has a 1-σ magnitude of 3 to 3.8 m/s. In this context the mean control metric distance of 14 m/s matches our intuition.

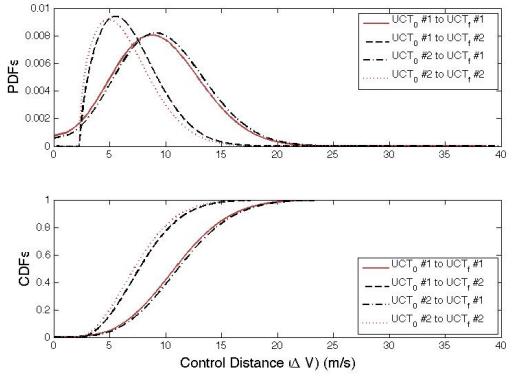

(a) Individual control distances in terms of ΔV

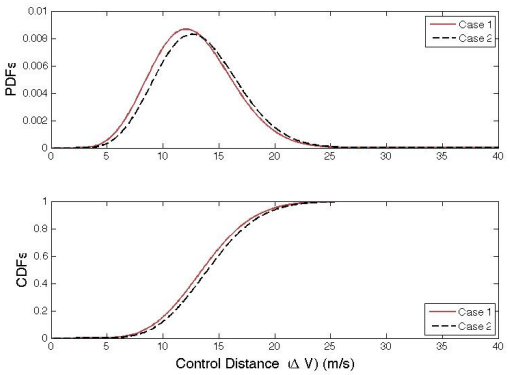

(b) Mutually exclusive control distances for cases 1 and 2 in terms of ΔV.

Figure 6: Control distance distributions for candidate connecting trajectories and mutually exclusive association cases

3.2 Scenario 2: Geostationary Maneuver Detection

Real-time maneuver detection is illustrated in this example by examining scenario in which a GEO spacecraft executes a small North-South maneuver to correct for an inclination error of 0.5 degrees. Simultaneously an observer is assumed to be filtering optical measurements of the object and propagating an estimate and covariance in real-time. To correct the spacecraft inclination error an impulsive maneuver immediately after time t_0 of $\Delta V = 26.8$ m/s is executed, unknown the observer. The maneuver occurs immediately after the observer's filter processes its last measurement. The time between the initial maneuver (which is also the time of the previous measurement and filter update) and the next measurement is $\Delta t = t_f - t_0 = 14$ hours. The satellite initial orbit elements are $\mathbf{oe}_0 = [a, e, i, \Omega, \omega, f] = [42086$ km, 0, 0.5 deg, 0 deg, 0 deg, 0 deg]. The state uncertainty of the geostationary satellite at time t_0 is $\sigma_x = 40$ m, $\sigma_y = 20$ m, $\sigma_z = 20$ m, $\sigma_{\dot{x}} = 3.0$ m/s, $\sigma_{\dot{y}} = 1.5$ m/s, and $\sigma_{\dot{z}} = 1.5$ m/s. The optical measurement uncertainty at the final time t_f is $\sigma_m = 10$ arcseconds. The observing ground station is located where the inertial x axis intersects the surface of the earth at time t_f. The measurement equation for the optical boresight azimuth β and elevation γ is then

$$\begin{bmatrix} \beta \\ \gamma \end{bmatrix} = \mathbf{y} = \mathbf{h}(\mathbf{x}) = \begin{bmatrix} \tan^{-1}\left(\frac{y}{\sqrt{(x-R_e)^2+y^2+z^2}}\right) \\ \tan^{-1}\left(\frac{z}{\sqrt{(x-R_e)^2+y^2+z^2}}\right) \end{bmatrix} \tag{8}$$

Because the measurement residual $\delta\mathbf{y} = \mathbf{y}_m - \mathbf{h}(\mathbf{x})$ is a random variable that is realized for each measurement (it is considered constant for each measurement and control metric distrubtion computation cycle), distributions corresponding to several residuals must be computed. To visualize this effect an approach from Unscented Kalman Filtering is adapted. The 1-sigma-points in the residual space are sampled and the corresponding control distance distribution is determined. The measurement residuals at time t_f are given in Table 4.

Table 4: Measurement residuals at $t_f = 14$ hours with maneuver ($\Delta V = 26.8$ m/s)

	nominal	σ-point 1	σ-point 2	σ-point 3	σ-point 4
$\delta\beta$ (rad)	0.000333	0.000333	0.000333	0.000382	0.000285
$\delta\gamma$ (rad)	0.00393	0.00398	0.00388	0.00393	0.00393

Fig. 7 plots Pearson's Approximation for both nominal and sigma-point residuals. The control distance distributions exhibit good control distance distributions, with the nominal residual generating a mean control

distance of $\mathbb{E}[\Delta V_{nom}]$ = 28.4 m/s. This is only marginally larger than the actual maneuver magnitude of ΔV = 26.8 m/s.

There are several reasons that the control distance distribution is conservative. First, the control distance distribution uses a quadratic cost and not a total ΔV performance index. As shown in (2), the ΔV plotted in Fig. 7 for the MRBVP is an upper bound for the true ΔV, so given a full state measurement the distribution will always be larger on average than the observable optimal impulsive maneuver. It is important to bear in mind that the new measurement does not measure the full state-space of the spacecraft, so while (2) suggests

The traditional approach to maneuver detection would compute the Mahalanobis distance of the pre-update residual. In the absence of process noise the covariance used to compute the Mahalanobis distance is $\text{Var}[\delta\mathbf{y}] = \mathbf{H}\mathbf{\Phi}_{xx}(t_f,t_0)\mathbf{P}_0\mathbf{\Phi}_{xx}(t_f,t_0)^T\mathbf{H}^T + \mathbf{R}$. In the nominal case with the ΔV maneuver, the Mahalanobis distance also exceedingly large, well into the region in which existing methods would detect the maneuver.

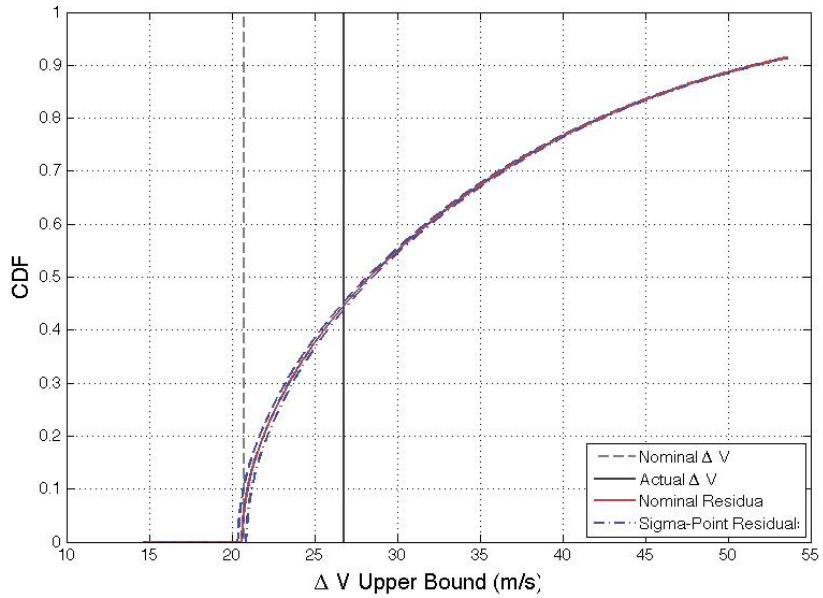

Figure 7: Control distance distribution Cumulative Distribution Functions (CDFs) in terms of ΔV. The vertical black line is the true maneuver magnitude. The red line is the distribution generated by the nominal residual, the blue lines are the 1-σ point distributions about the nominal residual, and the vertical grey line is the minimum connecting ΔV derived from the nominal residual (without accounting for measurement or state uncertainty.

4 CONCLUSION

In this paper the Uncertain Two Point Boundary Value Problem (UTPBVP) and the Measurement Residual Boundary Value Problem (MRBVP) are applied to object correlation and maneuver detection / characterization, respectively. The control distance metric P is introduced and it's property as an upper bound on the ΔV cost of an optimal maneuver is established. The UTPBVP and MRBVP approaches are summarized and the resulting control distance distributions are discussed. The utility and applications of each approach is emphasized. Two scenarios are introduced to illustrate how object correlation or maneuver detection may be used operationally. The first scenario examines a GEO spacecraft cross-tagging problem and demonstrates how control metric distances may be used to correlate UCTs. The second scenario accurately generates a control distance distribution given a single measurement after an observation gap. Future work includes

further improvement on the current performance metric distribution approximation and explicit use of ΔV performance metrics (rather than upper bounds or analogs).

ACKNOWLEDGEMENTS

This work was supported by AFOSR Grant No. FA9550-08-1-0460.

References

[1] L. James, "On Keeping the Space Environment Safe for Civil and Commercial Users," Statement of Lieutenant General Larry James, Commander, Joint Functional Component Command for Space, Before the Subcommittee on Space and Aeronautics, House Committee on Science and Technology, April 28, 2009.

[2] C. M. Cox, E. J. Degraaf, R. J. Wood, T. H. Crocker, "Intelligent Data Fusion for Improved Space Situational Awareness," AIAA Space 2005 Conference, Long Beach, 2005.

[3] D. Oltrogge, S. Alfana, R. Gist, "Satellite Mission Operations Improvements Through Covariance Based Methods," AIAA 2002-1814, SatMax 2002: Satellite Performance Workshop, 22-24 April 2002, Laurel, MD.

[4] T. S. Kelso, "Analysis of the Iridium 33-Cosmos 2251 Collision," Advanced Maui Optical and Space Surveillance Technologies Conference, September, 2009.

[5] A. B. Poore, "Multidimensional Asignment Formulation of Data Association Problems Arising from Multitarget and Multisensor Tracking," Computational Optimization and Applications, 3, pp. 27-57, Kluwer Academic Publishers, Netherlands, 1994.

[6] S. Kullback, "Information Theory and Statistics," John Wiley & Sons, Inc., New York, 1959.

[7] T. Kailath, "The Divergence and Bhattacharyya Distance Measures in Signal Selection," IEEE Transactions on Communication Technology, Vol. Com-15, No. 1., February 1967.

[8] M. J. Holzinger, D. J. Scheeres, "Object Correlation, Maneuver Detection, and Maneuver Characterization using Control Effort Metrics with Uncertain Boundary Conditions and Measurements," AIAA Conference on Guidance, Navigation, and Control, Toronto, August 2010.

[9] A. W. Naylor, G. R. Sell, "Linear Operator Theory in Engineering and Science," Applied Mathematical Sciences 40, Springer-Verlag, New York, NY, 2000.

[10] E. D. Gustafson, D. J. Scheeres, "Optimal Timing of Control-Law Updates for Unstable Systems with Continuous Control," Journal of Guidance, Control, and Dynamics, Vol. 32, No. 3, MayJune, 2009.

[11] B. D. Tapley, B. E. Schutz, G. H. Born, "Statistical Orbit Determination," Elsevier Academic Press, Inc, Amsterdam, 2004.

[12] A. M. Mathai, S. B. Provost, "Quadratic Forms in Random Variables: Theory and Applications," Marcel Dekker, Inc., New York, NY, 1992.

[13] A. Meucci, "Risk and Asset Allocation," 3rd Printing, Springer-Verlag, New York, NY, 2007.

[14] T. S. Kelso, "Two Years of International Cooperation on Conjunction Mitigation," 8^{th} US/Russian Space Surveillance Workshop, April, 2010.